Published in final edited form as:
Cell Mol Bioeng. 2011 June ; 4(2): 270–280. doi:10.1007/s12195-011-0160-4.

Whole-Cell Electrical Activity Under Direct Mechanical Stimulus by AFM Cantilever Using Planar Patch Clamp Chip Approach

Kalpesh V. Upadhye[1], **Joseph E. Candiello**[3], **Lance A. Davidson**[2], and **Hai Lin**[3]

[1]Department of Bioengineering, University of Pittsburgh, Suite 306, 300 Technology Drive, Pittsburgh, PA 15219, USA

[2]Department of Bioengineering, University of Pittsburgh, Bioscience Tower 3-5059, 3501 Fifth Avenue, Pittsburgh, PA 15260, USA

[3]Department of Bioengineering, University of Pittsburgh, Pittsburgh, PA, USA

Abstract

Patch clamp is a powerful tool for studying the properties of ion-channels and cellular membrane. In recent years, planar patch clamp chips have been fabricated from various materials including glass, quartz, silicon, silicon nitride, polydimethyl-siloxane (PDMS), and silicon dioxide. Planar patch clamps have made automation of patch clamp recordings possible. However, most planar patch clamp chips have limitations when used in combination with other techniques. Furthermore, the fabrication methods used are often expensive and require specialized equipments. An improved design as well as fabrication and characterization of a silicon-based planar patch clamp chip are described in this report. Fabrication involves true batch fabrication processes that can be performed in most common microfabrication facilities using well established MEMS techniques. Our planar patch clamp chips can form giga-ohm seals with the cell plasma membrane with success rate comparable to existing patch clamp techniques. The chip permits whole-cell voltage clamp recordings on variety of cell types including Chinese Hamster Ovary (CHO) cells and pheochromocytoma (PC12) cells, for times longer than most available patch clamp chips. When combined with a custom microfluidics chamber, we demonstrate that it is possible to perfuse the extra-cellular as well as intra-cellular buffers. The chamber design allows integration of planar patch clamp with atomic force microscope (AFM). Using our planar patch clamp chip and microfluidics chamber, we have recorded whole-cell mechanosensitive (MS) currents produced by directly stimulating human keratinocyte (HaCaT) cells using an AFM cantilever. Our results reveal the spatial distribution of MS ion channels and temporal details of the responses from MS channels. The results show that planar patch clamp chips have great potential for multi-parametric high throughput studies of ion channel proteins.

Keywords

On-chip patch clamp; MEMS; Atomic force microscopy; Whole-cell recordings; Mechanosensitive ion channels

Address correspondence to Kalpesh V. Upadhye, Department of Bioengineering, University of Pittsburgh, Suite 306, 300 Technology Drive, Pittsburgh, PA 15219, USA; Lance A. Davidson, Department of Bioengineering, University of Pittsburgh, Bioscience Tower 3-5059, 3501 Fifth Avenue, Pittsburgh, PA 15260, USA. kalpesh.upadhye@gmail.com, lad43@pitt.edu.

INTRODUCTION

All living cells have a plasma membrane that separates their interior compartments and the internal organelles from the surrounding environment. The membrane consists of a lipid bilayer which prevents passage of ions and macromolecules across the cell boundaries. Specialized proteins in the cell membrane, such as ion-channels and other transporters, mediate the transport of ions and small polar molecules including sugars and amino acids, in and out of the cell. A number of different ion channels are present on the cell membrane, including passive pores, as well as voltage sensitive, ligand-gated, and mechano-sensitive gating proteins.[12] Ion channels help maintain the crucial ionic balance inside cells and mediate communication and the electrical signaling within cells and tissues in the nervous system, heart, and other organs via ionic currents conducted through various ionchannels. Ion channels have also been important targets for therapeutic intervention for a wide variety of diseases.[3,6,24]

The most powerful tool for studying ion-channel properties is the “patch-clamp” technique.[12] In conjunction with molecular biology techniques used to modify the expression of ion channels in a cell the patch clamp technique has, over the years, been used to glean much useful information about the mechanisms underlying ion channel activity. In the conventional patch clamp, the electrode is connected to the cell membrane via an electrolyte filled glass micropipette. The micrometer-sized pipette opening forms a tight seal (giga-ohm resistance) with the cell membrane. The cell is then clamped to a voltage signal and ionic current across the sealed small membrane patch or the entire cell is measured.

Patch clamp experiments have traditionally been laborious and have required skillful manipulation of a micropipette to make delicate contact with the cell plasma membrane. Only one cell can be probed at a time and access to the cell for any other probing technique is restricted. The architecture of the experiment allows only the extra-cellular buffer to be easily changed to add or remove pharmacological agents useful to the study. These limitations have slowed the progress in the understanding of ion channel physics and there have been considerable efforts to make the patch clamp process more compatible with automation and high throughput ion channel screening.[36,38]

Several groups have developed planar patch clamps in the form of a micron sized aperture in a microfabricated chip, using different materials such as quartz,[8,9,39] silicon,[32,37] silicon nitride,[35] Teflon,[26] and polydimethyl-siloxane (PDMS).[16,18] Recently, nonplanar forms of multiple-patch chip made of PDMS have been developed and these PDMS-based chips allow simultaneous patch recording from multiple cells and fluorescence microscopy imaging.[5,16,23] The PDMS-based planar devices were built using micromolding process,[18] whereas quartz, silicon, and silicon nitride based planar patch clamps were made using semiconductor fabrication methods. Compared to glass pipettes, planar patch clamps can have significantly better electrical characteristics due to their lower serial resistance and capacitance. Furthermore, fabrication of planar patch clamp chips involves batch processing techniques used in semiconductor industry resulting in highly consistent devices. Sigworth and Klemic[36] provide a good review of the planar patch clamp technologies.

Atomic force microscope (AFM) is a powerful tool for measuring and applying small forces over small areas. The primary advantage of AFM stems from the sub-nanometer resolution it can provide in physiological conditions. AFM has been used for measuring mechanical properties of tissues by indenting the tissue with known forces under physiological conditions. AFM can be used to apply forces as small as 1 nN and perform indentations on the order of nanometers on live cells[4,27] at rates ranging from 10 nm/s to 10 μm/s. AFM imaging of the plasma membrane of live cells is straight forward and has provided useful

information about ion channels, cellular processes and dynamics. [20,21,25,33] For instance, AFM images of excised membrane patches spanning the opening of a glass pipette have been obtained.[13,22] Movement of the cell membrane in response to voltage stimuli have been shown in pipette based patches.[40] Whole-cell membrane responses to voltage stimuli have been reported in the seminal work by Benoit *et al*. in a chip-based system.[31] It has also been shown using pipette patches that voltage induced movement activates mechanosensitive (MS) channels.[11] AFM has also been used in conjunction with conventional micropipettes to study electromechanical coupling in cell membranes.[2] But so far, to the best of our knowledge, the use of AFM to provide controlled mechanical stimuli to compliment chip-based electrophysiology in studying activation dynamics of MS ion channels in live cells has not been reported.

This communication reports the fabrication of a planar patch clamp chip and related microfluidics that can be integrated with high resolution optical microscopy and AFM. A circular, micron-sized aperture was etched into thermally oxidized silicon on undoped silicon wafer, which makes up the substrate. The chip was then etched from the backside to form a silicon dioxide membrane with a pore. Thermally oxidized silicon, being essentially quartz, provided excellent dielectric properties to the chip. The flat, thin membrane ensured that a cell clamped on top of the chip could be visualized from the underside using an optical microscope. The fabrication process yielded a smooth, circular pore that was necessary for providing good cell adhesion and a giga-ohm seal in order to perform whole-cell recordings. Giga-ohm seals with the cellular membranes of multiple kinds of cells have been achieved. A microfluidic chamber was custom built for this study. The chamber design provided easy access to the cell for a probe such as a cantilever of an AFM from the top side. Exchange of the extra-cellular and intra-cellular buffers while performing whole-cell electrical recordings was also possible in this design. A proof of principle for the exchange of buffers was demonstrated using perforated patch recordings performed on Chinese Hamster Ovary (CHO) cells.

This study concludes by recording whole-cell current from single HaCaT keratinocyte cells while being probed by an AFM cantilever. The results reveal, for the first time, the spatial distribution of MS channels across the surface of a HaCaT cell. It was observed that MS channels are distributed non-uniformly, possibly in clusters across the cell membrane. The wealth of knowledge that can be gained by integrating AFM with cellular electrophysiology has already been demonstrated. [2,13,28,31,40] These results further enhance that knowledge by demonstrating the potential of our apparatus to perform multi-parametric investigation of MS ion channels in mammalian cells.

MATERIALS AND METHODS

Chip Fabrication

Double-sided polished 400 μm thick (100) silicon wafers (Universal Wafers, South Boston, MA) with 1 μm thick thermally grown oxide were used for fabricating the chip (Fig. 1a). After cleaning the wafers, electron-beam resist polymethyl methacrylate (PMMA; Microchem, Corp., Newton, MA) was spincoated on one side (top-side for the device) using a programmable spinner at 4000 rpm and baked at 95 °C for 10 min. Apertures with 1.5 μm diameter were then patterned with PMMA using an electronbeam lithography system (Raith GmbH, Dortmund, Germany) and developed in a pre-mixed methyl isobutyl ketone (MIBK) developer (Microchem, Corp., Newton, MA). Photoresist AZ4210 (Shipley Co., Inc., Marlborough, MA) was spin-coated (3000 rpm) on the other side (bottom-side for the device) of the wafer and baked at 90 °C for 15 min. Circular apertures of 100 μm diameter aligned so as to keep the apertures from the top-side at the center of these circles on the under-side and patterned using a double-sided mask aligner (Karl Suss, Germany). This

pattern was developed (Fig. 1c) using a pre-mixed developer specific to AZ4210 (Shipley Co., Inc.). Silicon dioxide (top and bottom) was then etched in a carefully timed reactive ion etching (RIE) step (Trion Technology, Clearwater, FL) using a mixture of CHF_3, Ar, and O_2 gases. Both the resists were then dissolved in acetone (Fig. 1d) and the silicon substrate was etched through from bottom-side (Fig. 1e) using xenon difluoride (XeF_2) isotropic dry etching process (Xactix, Inc., Pittsburgh, PA). Each wafer had a 1 × 1 cm array of devices having a 1 μm thick, 100 μm diameter circular silicon dioxide membrane with a 1.5 μm diameter aperture in its center. The silicon dioxide membrane was visible from the bottom-side of the device.

Design and Fabrication of the Perfusion Chamber

The perfusion chamber was designed to provide easy access to probe the top side of the cell while at the same time maintaining electrical contact through the bottom surface. The electrical separation of the top and bottom sides of the chip was achieved with an O-ring on the bottom side of the chip (Fig. 1f). The chamber was designed to seat the chip on a small circular reservoir, 8 mm in diameter and 0.4 mm deep, with three feed lines (1 mm in diameter) connecting to the reservoir. Two of the feed lines served to exchange the intracellular buffer and the third to hold the recording electrode. The assembly had another piece that pressed on the chip from top with another O-ring and three feed lines similar to the ones on the bottom piece (Fig. 1g). The ultra thin rubber O-rings for the assembly were obtained from Apple Rubber Products, Inc. (Lancaster, NY). The electrode on the top side acted as the extra-cellular ground electrode while recording from the cell whereas the one electrode in the bottom reservoir served as the intra-cellular recording electrode (see Fig. 1f for schematic).

Chamber and chip designs were further constrained to leave the top of the chip free of obstruction and make the bottom of the chamber as thin and transparent as possible while still allowing space for electrodes. The width of the chip-holder was dictated by the cantilever holder of our AFM (MFP-3D by Asylum Research, Santa Barbara, CA) and the thickness of the bottom side reservoir of the chamber was constrained by the working distance of our optical microscope (inverted Olympus IX71).

The chamber was designed with the 3D modeling software SolidWorks™ at the department of bioengineering computing facility and fabricated using 3D stereolithography (3-D Systems SLA250 stereolithography apparatus) at the John A. Swanson Center for Product Innovation, University of Pittsburgh. The photopolymer WaterShed XC 11122 by DSM Somos (Elgin, IL), was used to fabricate the chamber because of its low viscosity (for the high resolution necessary), high transparency (RI: 1.15) and excellent mechanical properties.

Cell Culture

Chinese Hamster Ovary (CHO), pheochromocytoma (PC12) and human keratinocytes (HaCaT) were used to study the characteristics of our device. All cells were cultured at 37 °C with 5% ambient CO_2 in 76 mm culture dishes. CHO cells were grown in Ham's F12 media (Sigma-Aldrich, St. Louis, MO) with 10% fetal bovine serum (FBS) (GIBCO, Carlsbad, CA) and 1% (v/v) antibiotic–antimycotic solution (10 mg/mL Penicillin, 10 mg/mL Streptomycin and 25 μg/mL Amphotericin B; Mediatech, Inc., Manassas, VA). PC12 cells were grown in DMEM media (Sigma-Aldrich) with 5% FBS and 1% antibiotic–antimycotic solution and HaCaT cells were grown in DMEM media with 10% FBS and 1% antibiotic–antimycotic solution.

An important pre-requisite for good quality electrical recordings is that the media containing target cells be free of any solid non-cellular material. In order to achieve this, we developed

a simple protocol to extract cells from the culture. Briefly, the culture medium aspirated from the dish and after rinsing the cells three times with phosphate buffered saline (PBS) 2 mL of 0.25% trypsin–EDTA solution added to the dish and incubated at 37 °C for 5 min. After gentle agitation, the trypsin–EDTA solution was aspirated out into a centrifuge tube and 3 mL of culture medium was added to the tube to inhibit trypsin activity. The culture dish was refilled with 10 mL of culture medium and replaced in the incubator. The tube with cells was centrifuged at 10,000 rpm for 4 min and the supernatant was removed and discarded. After adding 3 mL of PBS to the cellular pellet remaining behind in the tube, the trypsin treatment was repeated for 2 min to ensure that all the extra-cellular debris was hydrolyzed. A small amount of the suspension was observed under a phase-contrast microscope to check for debris. If any debris was observed Trypsin treatment was repeated for smaller amounts of time until no debris was seen in the suspension. The shorter subsequent trypsin treatments (if necessary) ensured that the extracellular domains of membrane proteins remained unaffected by trypsin. Finally, the cells were suspended in isotonic extra-cellular buffer necessary with sufficient dilution for the specific experiment.

Electrophysiology

For whole-cell recordings, a commercially available patch-clamp amplifier (model 2400, A-M Systems, Carlsborg, WA) and the shareware electrophysiology data acquisition software (WinWCP v3.5.6, Strathclyde Electrophysiology Software, Strathclyde Institute of Pharmacy and Biomedical Sciences, University of Strathclyde, UK) on a standard PC (Dell, Inc., Round Rock, TX) with National Instruments (Austin, TX) PCI-6070E multifunction data acquisition card was used. The data was sampled at 10 kHz and filtered at 2 kHz. All the data acquired was archived on the hard-drive of the PC. The intracellular buffer (on the bottom side of the chip) used for the electrical recordings consisted of 125 mM KCl, 2 mM $CaCl_2$, 1 mM $MgCl_2$, 10 mM EGTA, and 5 mM HEPES. The final free Ca^{2+} concentration was ~1 μM at a pH of 7.4. Basal Media Eagle's (Sigma-Aldrich) without the pH indicator was used as extracellular buffer (on the top side of the chip). The same buffers were used for all of cells unless specifically stated otherwise. The chip was used as a replacement for the micropipette to perform the patch-clamp experiments. Ag/AgCl electrodes from the top and bottom sides of the perfusion chamber were connected to the patch-clamp amplifier.

AFM

An AFM (MFP-3D, Asylum Research, Santa Barbara, CA) head mounted on the stage of an inverted compound microscope (Olympus IX71) was used to perform the experiments (Fig. 1f). Standard commercially available 100 μm long silicon nitride cantilevers with a nominal spring constant of 0.1 N/m were used for our experiments. The AFM cantilever was calibrated using the thermal fluctuation method.[15] The perfusion chamber and chip assembly was placed on the microscope stage with appropriate buffers. About 500 μL of the cell suspension was placed on the top side of the chip and the cell was patched using the protocol mentioned above. The AFM head was then placed on top of the chamber and the cantilever aligned over the patched cell. This was achieved by moving the stage while observing the cell with the microscope. Once the cell and the cantilever were aligned, we used the AFM control software to indent the patched HaCaT cell at 100 locations on a 10 × 10 grid over a 5 × 5 μm area while simultaneously recording the whole cell current through the cell. The automated indentations were carried out using the cFVol software program (Chad Ray, Duke University, Durham, NC, USA) within the MFP-3D control software, at a rate of one load/unload cycle per second. The cell was held at −70 mV throughout the 10 min time-course of the scan. Deflection data from the AFM was collected by a data acquisition card (National Instruments, Corp., Austin, TX) synchronized with the data from the patchamplifier, and stored on the computer.

RESULTS AND DISCUSSION

Characterization of the Chip

Scanning electron micrograph of the top side of the chip shows a circular pore in the silicon dioxide membrane (Fig. 2b). The open-pore resistance, resistance between the top and bottom electrodes with the respective buffers present but not the cell, is a good indicator of the quality of the pore. The resistance is proportional to the depth of the pore and inversely proportional to the square of its radius. For a 1 μm deep pore with a diameter of 1.5 μm, the open pore resistance would be ~1 MΩ depending on the temperature and the precise contents of the buffer being used. Chips with open-pore resistances of 3 MΩ or higher were discarded for quality control.

The bottom reservoir of the perfusion chamber was filled with the intra-cellular solution while ensuring that there were no air-bubbles, the chip was placed on the reservoir after wetting the pore properly and the top half of the chamber was sealed onto the chip. The cell suspension was then added to the top side of the chip. While the cells settle for about 30 s, gentle pressure was applied from the bottom side to keep any possible small particle contaminants away from the pore. The pressure was then switched to a gentle suction to draw the cell to the pore. The resistance across the pore was simultaneously monitored. The suction was stopped after the resistance saturated (leading to the cell-attached configuration) to a high value (100 s of MΩ to GΩ) and a sharp, more intense suction pulse was applied from the bottom side to rupture the patch of membrane sealed in the pore, thus giving access to the inside of the cell and forming a whole-cell patch. The whole process took less than 2 minutes. While a microscope is not needed during the process, the perfusion chamber design allowed imaging by an inverted, reflecting optical microscope from the under-side. The cell patched on the chip pore could be observed from the bottom side of the chamber with an optical microscope (Fig. 2a).

The cell-attached seal resistance was measured for PC12 and CHO cells. Chips showing resistances < 100 MΩ were discarded as leaky patches. Of the 57 chips tested, seal resistance of > 1 GΩ was achieved in eight cases (Fig. 2c). The maximum seal resistance achieved was 1.22 GΩ. It was observed that chips having higher open-pore resistance generally yielded higher seal resistance.

Obtaining giga-seal is highly dependent on the specific cell type, the nature of the pore, the quality of the cells and several other factors. The success rate (of about 14%) in obtaining giga-seals in our apparatus could be improved. The pressure changes in this setup were achieved manually using a syringe. We believe that a more automated application of pressures using syringe pumps will certainly improve the success rate and consistency in obtaining giga-ohm seals with our chips.

Whole Cell Recordings

The ultimate determinant of efficacy of the chip is how well we can measure whole-cell currents from live cells. In order to test this, we used CHO and PC12 cells to perform whole-cell recordings. We were able to successfully record whole-cell currents from CHO (n = 9) and PC12 (n = 16) cells choosing from chips which provided >600 MΩ seal resistance. Instances with seal resistance <600 MΩ were considered to be leaky seals; hence, no whole-cell recording was attempted. The cell membrane potential was clamped at −70 mV for both types of cells. The observed current response to voltage steps was consistent with the literature[7,10] (Fig. 3a for CHO and Fig. 3c for PC12).

As proof of principle for our ability to exchange buffers, PC12 cells were used to perform potassium blocking and recovery experiments by adding Ba^{2+}, a selective, non-specific and

reversible blocker of certain types of K^+ channels[1] to the extra-cellular solution. PC12 cells express several types of K^+ channels.[14] The *I–V* relationship of a PC12 cell in whole-cell configuration before (Fig. 3c; squares) and after (Fig. 3c; solid circles) the addition of 1 mM $BaCl_2$ to the extracellular solution shows a noticeable reduction in whole-cell current after the addition of Ba^{2+}. The reversal potential of the Ba^{2+}-sensitive current (Fig. 3c inset) is approximately −72 mV, which is close to the K^+ equilibrium potential under our experimental conditions (the experimental Nernst potential $E_K = \frac{RT}{F} \ln \frac{[K^+]_{out}}{[K^+]_{in}} \approx -81$ mV, $[K^+]_{out}$ = 5.3 mM, $[K^+]_{in}$ = 125 mM, and T = 25 °C, R and F are gas constant and Faraday constant, respectively). The difference between the calculated and measured reversal potential is attributed to the presence of un-blocked K^+ channels present in PC12 cells as well as to the leak current from the cells.

The CHO and PC12 cells used in these experiments were from wild-type cell lines. Unmodified CHO cells are not known to express any voltage sensitive channels, [10] thus, a fairly linear response from these cells is expected. Unmodified PC12 cells, on the other hand express a variety of calcium-selective channels, sodium channels, chloride channels, ligand gated channels as well as a small number of voltage sensitive ion channels [7] but are not known to be electrically excitable unless stimulated by nerve growth factor.[17] This explains the lack of rectifying response in these PC12 cells. K^+ is not the majority charge carrier in PC12 cells, but blocking K^+ current does reduce the outward current by a measurable degree as seen in the *I–V* plot (Fig. 3c). These results demonstrate the capability of our apparatus to allow for exchange of extra-cellular buffer.

Perforated Patch Recordings on CHO Cells

In order to demonstrate our ability to exchange the intra-cellular buffer with pharmacological agents of interest, we introduced amphotericin B into the bottom-side reservoir of the chamber. Amphotericin B is known to form large non-selective cation channels in cell membrane[34] resulting in the so-called perforated patch. Higher resistance than that offered by the cell in the whole-cell configuration is expected in the perforated patch configuration. Voltage pulses increasing step-wise were applied to a CHO cell in cell-attached configuration 5 min after perfusing amphotericin B (200 μg/mL) and the current response was recorded. The current response to voltage steps (Fig. 3b) clearly shows that the *I–V* characteristics in this case are quite similar to the whole-cell configuration with the exception of the resistance offered. Resistance in this case is higher (about 18 MΩ) compared to what is observed in the whole-cell configuration (about 5–6 MΩ) (Fig. 3a).

Recordings have been possible from a patched cell for as long as 90 min (at room temperature), beyond which time, the signal is lost and resistance reverts back to open-pore value. It was assumed that at this time the cells either die or the seal was broken. Nearly 700 cells have been recorded from using this setup and about 87% of these lasted for more than 40 min. About 61% of the whole-cell patches were stable for as long as 65 min and about 26% of the cells could be recorded between 65 and 90 min and exactly 23 whole-cell patches were stable for 85 to 90 min. The 13% of the records that lasted for less than 40 min were found to have relatively poor seal resistances and it is possible that the cells were alive for longer periods, but floated away as the seal was broken.

Current Response to Mechanical Stimuli

Chip-based planar patch clamp approach has the potential to provide a stable platform for electrophysiology with direct mechanical stimulus using equipment such as an AFM. We attempted to integrate our planar patch clamp assembly with an AFM and an optical microscope.

The distribution of MS channels across the cell membrane is unknown. The probability of getting a current response from an indentation at any given spot is, therefore, unknown. In order to address this problem, we performed an array of indentations over a 5 × 5 μm area on HaCaT cells which are known to express TRPV4 channels. The cells were voltage clamped at 0 mV to ensure that the current through MS channels is purely because of the chemical potential of the respective ions. Long thin triangular silicon nitride cantilevers with a nominal spring constant of about 0.1 N/m were used for these experiments. The radius of curvature of the pyramidal cantilever tip was on the order of nanometers. A 10 × 10 grid was chosen so that two consecutive indentation points are 500 nm apart which would be sufficiently long to avoid overlap of area affected by neighboring indentations, given the cantilever parameters. An indentation depth of about 30 nm was chosen based on previous studies[19,30] to ensure that the force applied does not penetrate the membrane. Visual analysis of the force curves found that there were no penetration events for indentation depths of up to 45 nm. The distribution of MS channels can be, thus, mapped by recording currents at each indentation point. The current values obtained from indenting the 10 × 10 grid on the cell are represented in grey-scale (large current indicated by white and low current indicated by black pixels; Fig. 4a) with the largest current being shown by the brightest pixel. Each indentation is represented by the voltage measured across the photodiode as the cantilever deflects while indenting the cell. We define some kinetic parameters for the current response in the representation of photodiode voltage corresponding to high resolution view of the current response from a single indentation (Fig. 4c):

- *t*(indent): time over which the cantilever is in contact with the cell membrane;
- *t*(1/2): time between the onset of the current and the current-reading peak value;
- *t*(peak_lag): time between the maximum indentation depth and current peak;
- *t*(delay): time between membrane contact and the onset of current;
- *t*(open): time over which the channels are open.

From the current response (labeled HaCaT in Fig. 4a), it is apparent that MS channels are not uniformly distributed over the cellular surface, the current is inward and varies for consecutive indentations. We attribute this inward current to calcium flowing into the cell through MS channels (most likely TRP-family channels TRPV4 and TRPC6) present on the HaCaT cells that are activated by mechanical stimulus provided by the AFM cantilever. In order to test this hypothesis, we added 1 mM Gd^{3+} (a known blocker for several calcium-selective MS channels, but not voltage or ligand gated channels) to the extra-cellular solution and found that the current response seen in HaCaT cells was eliminated. As a control, we repeated the experiment with a CHO cell as control and found that indentations did not induce any response from CHO cells (Fig. 4b).

The maximum current from a single indentation was found to be about 110 pA. Assuming an average single channel current of about 5 pA (comparable to TRPV4 single channel current of 3.7 pA[29]), we estimate that these MS channels are present in clusters and one indentation can activate about 25 or fewer channels at once depending on the site of indentation.

It is important for a patch clamp setup, especially in case of micromanipulator clamped micropipettes, to be insensitive to vibrations in order to maintain the integrity of the patch. It was even more important for our experiments because of the potential of mechanical vibrations to induce electrical response, and hence noise in our measurements. In terms of whole-cell patch, our setup was found to be insensitive to mechanical vibrations; vibration isolation of any kind was not necessary while recording whole-cell currents. We believe that

this was possible because the cell lays flat on our chip and adheres to the surface around the pore, lending stability to the patch. Nevertheless, for the purpose of our experiments involving stimulation by AFM, the entire setup was mounted on an active vibration isolation platform to damp out any vibrations and rid the system of mechanical noise.

CONCLUSION

We show, for the first time, whole cell electrical activity in live HaCaT cells in response to direct mechanical stimulus using an AFM cantilever. We achieve this by integrating a planar patch clamp chip with an AFM after a carefully optimized design of the chip as well as allied microfluidics. This electrical activity can be attributed to MS ion channels (predominantly TRPV4 in case of HaCaT cells) present on the cell.

We have mapped the distribution of MS channels on a HaCaT cell surface using this tool and found that MS channels are not uniformly distributed over the cell surface. The reason for this non-uniform distribution is a matter of further study. Distribution of various ion channels over the cell surface as well as within the cell have been studied using immuno-staining (fluorescent tags for optical microscopy or heavy metal tags for electron microscopy). However, a functional mapping of MS ion channels in live cells has not been reported.

The kinetic data obtained from recording current response to single indentations by the AFM cantilever tip can be used to fill existing gaps in models for the structure–function interactions as well as gating dynamics in MS channels. The miniaturized design of the patch clamp chip assembly reduces the capacitive delays in recording current responses making the kinetic data obtained more valuable. The apparatus can be extended to study the distribution of ligandgated ion channels by tagging the AFM cantilever tip with various agonists to map the distribution of specific channels.

In summary, our planar patch clamp chip assembly facilitates electrophysiology not only by automating the cell patching process, but by allowing fast exchange of intracellular as well as extracellular buffers. Low volumes of required buffers also reduce noise and capacitive delays. This chip-based approach can be extended to high-throughput electrophysiology screening by making specific changes in microfluidics to allow multiplexed parallel recording from an array of chips. The planar nature of our chip-based device allows for integration with optical and AFMs facilitating multi-parametric studies of ion channel dynamics thus opening up the possibility for a whole new class of experiments specifically for studying MS ion channels.

Acknowledgments

The authors would like to acknowledge the support provided by the John A. Swanson Center for Micro and Nano Systems and the Nanofabrication and Characterization Facility at the Petersen Institute of Nanoscience and Engineering for fabrication of the chip, John A. Swanson Center for Product Innovation for fabrication of the microfluidics and Center for Biological Imaging for electron microscopy. We would like to thank Prof. Ratneshwar Lal from University of California, San Diego and Prof. Sanjeev Shroff from University of Pittsburgh for their valuable advice and inputs. We are grateful to Prof. Elias Aizenman from the Department of Neurobiology of University of Pittsburgh School of Medicine for providing the CHO and PC12 cells as well as Prof. Chuanyue Wu from the Department of Pathology of University of Pittsburgh School of Medicine for providing the HaCaT cells. The research was supported by grants from NIH (R21-EB004474) and the Central Research Development Fund (CRDF) and startup fund from University of Pittsburgh.

References

1. Armstrong CM, Swenson RP Jr, et al. Block of squid axon K channels by internally and externally applied barium ions. J Gen Physiol. 1982; 80(5):663–682. [PubMed: 6294220]

2. Beyder A, Sachs F. Electromechanical coupling in the membranes of Shaker-transfected HEK cells. Proc Natl Acad Sci USA. 2009; 106(16):6626–6631. [PubMed: 19366664]
3. Cahalan MD, Chandy KG. Ion channels in the immune system as targets for immunosuppression. Curr Opin Biotechnol. 1997; 8(6):749–756. [PubMed: 9425667]
4. Candiello J, Balasubramani M, et al. Biomechanical properties of native basement membranes. FEBS J. 2007; 274(11):2897–2908. [PubMed: 17488283]
5. Chen C, Folch A. A high-performance elastomeric patch clamp chip. Lab Chip. 2006; 6(10):1338–1345. [PubMed: 17102847]
6. Clapham DE. TRP channels as cellular sensors. Nature. 2003; 426(6966):517–524. [PubMed: 14654832]
7. Dichter MA, Tischler AS, et al. Nerve growth factor-induced increase in electrical excitability and acetylcholine sensitivity of a rat pheochromocytoma cell line. Nature. 1977; 268(5620):501–504. [PubMed: 329148]
8. Fertig N, Blick RH, et al. Whole cell patch clamp recording performed on a planar glass chip. Biophys J. 2002; 82(6):3056–3062. [PubMed: 12023228]
9. Fertig N, George M, et al. Microstructured apertures in planar glass substrates for ion channel research. Recept Channels. 2003; 9(1):29–40. [PubMed: 12825296]
10. Gamper N, Stockand JD, et al. The use of Chinese hamster ovary (CHO) cells in the study of ion channels. J Pharmacol Toxicol Methods. 2005; 51(3):177–185. [PubMed: 15862463]
11. Gil Z, Silberberg SD, et al. Voltage-induced membrane displacement in patch pipettes activates mechanosensitive channels. Proc Natl Acad Sci USA. 1999; 96(25):14594–14599. [PubMed: 10588750]
12. Hille, B. Ion Channels of Excitable Membranes. Massachusetts: Sinauer Associates; 2001.
13. Horber JK, Mosbacher J, et al. A look at membrane patches with a scanning force microscope. Biophys J. 1995; 68(5):1687–1693. [PubMed: 7612812]
14. Hoshi T, Aldrich RW. Voltage-dependent K^+ currents and underlying single K^+ channels in pheochromocytoma cells. J Gen Physiol. 1988; 91(1):73–106. [PubMed: 2449514]
15. Hutter JL, John B. Calibration of atomic-force microscope tips. J Rev Sci Instrum. 1993; 64:1868–1873.
16. Ionescu-Zanetti C, Shaw RM, et al. Mammalian electrophysiology on a microfluidic platform. Proc Natl Acad Sci USA. 2005; 102(26):9112–9117. [PubMed: 15967996]
17. Janigro D, Maccaferri G, et al. Calcium channels in undifferentiated PC12 rat pheochromocytoma cells. FEBS Lett. 1989; 255(2):398–400. [PubMed: 2551740]
18. Klemic KG, Klemic JF, et al. Micromolded PDMS planar electrode allows patch clamp electrical recordings from cells. Biosens Bioelectron. 2002; 17(6–7):597–604. [PubMed: 11959483]
19. Kwon E-Y, Kim Y-T, Kim D-E. Investigation of penetration force of living cell using an atomic force microscope. J Mech Sci Technol. 2009; 23:1932–1938.
20. Lal R, Kim H, et al. Imaging of reconstituted biological channels at molecular resolution by atomic force microscopy. Am J Physiol. 1993; 265(3 Pt 1):C851–C856. [PubMed: 8214041]
21. Lal R, Lin H. Imaging molecular structure and physiological function of gap junctions and hemijunctions by multimodal atomic force microscopy. Microsc Res Tech. 2001; 52(3):273–288. [PubMed: 11180620]
22. Larmer J, Schneider SW, et al. Imaging excised apical plasma membrane patches of MDCK cells in physiological conditions with atomic force microscopy. Pflugers Arch. 1997; 434(3):254–260. [PubMed: 9178623]
23. Lau AY, Hung PJ, et al. Open-access microfluidic patch-clamp array with raised lateral cell trapping sites. Lab Chip. 2006; 6(12):1510–1515. [PubMed: 17203154]
24. Li S, Westwick J, et al. Transient receptor potential (TRP) channels as potential drug targets in respiratory disease. Cell Calcium. 2003; 33:551–558. [PubMed: 12765700]
25. Lin H, Bhatia R, et al. Amyloid beta protein forms ion channels: implications for Alzheimer's disease pathophysiology. FASEB J. 2001; 15(13):2433–2444. [PubMed: 11689468]
26. Mayer M, Kriebel JK, et al. Microfabricated teflon membranes for low-noise recordings of ion channels in planar lipid bilayers. Biophys J. 2003; 85(4):2684–2695. [PubMed: 14507731]

27. Merryman WD, Liao J, et al. Differences in tissue-remodeling potential of aortic and pulmonary heart valve interstitial cells. Tissue Eng. 2007; 13(9):2281–2289. [PubMed: 17596117]
28. Mosbacher J, Langer M, et al. Voltage-dependent membrane displacements measured by atomic force microscopy. J Gen Physiol. 1998; 111(1):65–74. [PubMed: 9417135]
29. Nilius B, Vriens J, et al. TRPV4 calcium entry channel: a paradigm for gating diversity. Am J Physiol Cell Physiol. 2004; 286(2):C195–C205. [PubMed: 14707014]
30. Obataya I, Nakamura C, et al. Mechanical sensing of the penetration of various nanoneedles into a living cell using atomic force microscopy. Biosens Bioelectron. 2005; 20(8):1652–1655. [PubMed: 15626623]
31. Pamir E, George M, et al. Planar patch-clamp force microscopy on living cells. Ultramicroscopy. 2008; 108(6):552–557. [PubMed: 17933465]
32. Pantoja R, Nagarah JM, et al. Silicon chip-based patch-clamp electrodes integrated with PDMS microfluidics. Biosens Bioelectron. 2004; 20(3):509–517. [PubMed: 15494233]
33. Quist AP, Chand A, et al. Atomic force microscopy imaging and electrical recording of lipid bilayers supported over microfabricated silicon chip nanopores: lab-on-a-chip system for lipid membranes and ion channels. Langmuir. 2007; 23(3):1375–1380. [PubMed: 17241061]
34. Rae J, Cooper K, et al. Low access resistance perforated patch recordings using amphotericin B. J Neurosci Methods. 1991; 37(1):15–26. [PubMed: 2072734]
35. Schmidt C, Mayer M, et al. A chip-based biosensor for the functional analysis of single ion channels. Angew Chem Int Ed Engl. 2000; 39(17):3137–3140. [PubMed: 11028058]
36. Sigworth FJ, Klemic KG. Microchip technology in ion-channel research. IEEE Trans Nanobiosci. 2005; 4(1):121–127.
37. Stett A, Bucher V, et al. Patch-clamping of primary cardiac cells with micro-openings in polyimide films. Med Biol Eng Comput. 2003; 41(2):233–240. [PubMed: 12691447]
38. Wang X, Li M. Automated electrophysiology: high throughput of art. Assay Drug Dev Technol. 2003; 1(5):695–708. [PubMed: 15090242]
39. Xu J, Guia A, et al. A benchmark study with sealchip planar patch-clamp technology. Assay Drug Dev Technol. 2003; 1(5):675–684. [PubMed: 15090240]
40. Zhang PC, Keleshian AM, et al. Voltage-induced membrane movement. Nature. 2001; 413(6854): 428–432. [PubMed: 11574890]

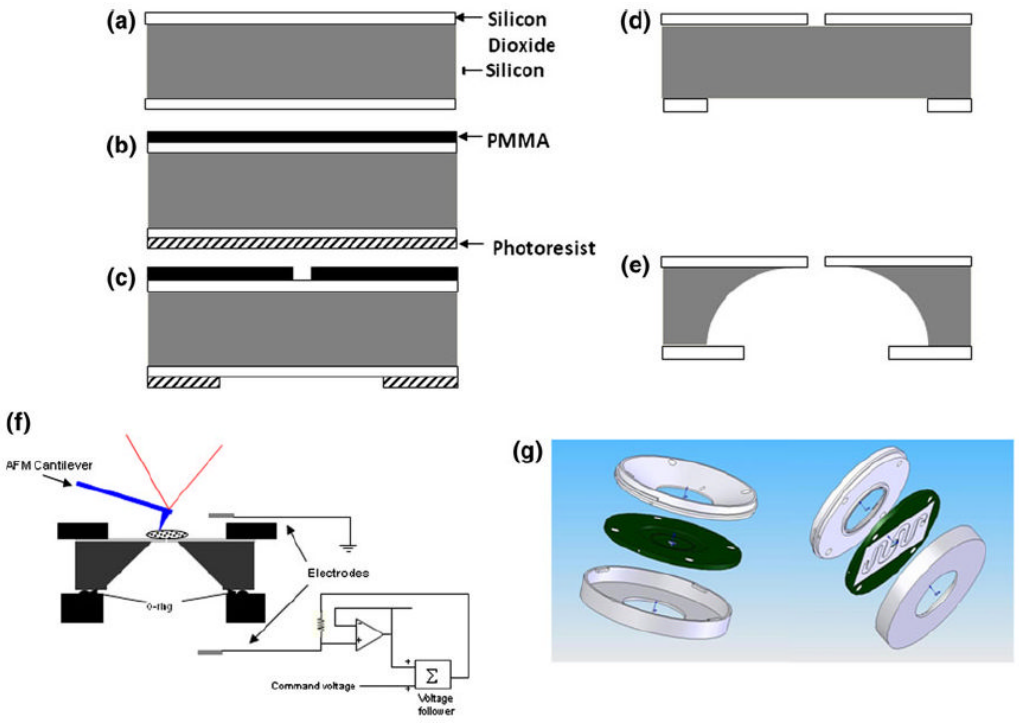

FIGURE 1.

Fabrication of the planar patch clamp chip, microfluidics chamber and integrated apparatus: (a) Oxidized silicon wafer was used as the starting material. (b) PMMA and photoresist were spin-coated on the top and the bottom, respectively. (c) 1 μm circles were defined in PMMA using electron beam lithography and circles of about 50 μm were defined, aligned to the top circles from the back of the wafer in the photoresist using photolithography. (d) Silicon dioxide was anisotropically etched using RIE; PMMA and photoresist were then removed. (e) Silicon was etched isotropically using a dry XeF_2 based process. (f) Schematic cross-section of the liquid cell (not to scale). (g) SolidWorks drawing of the liquid cell.

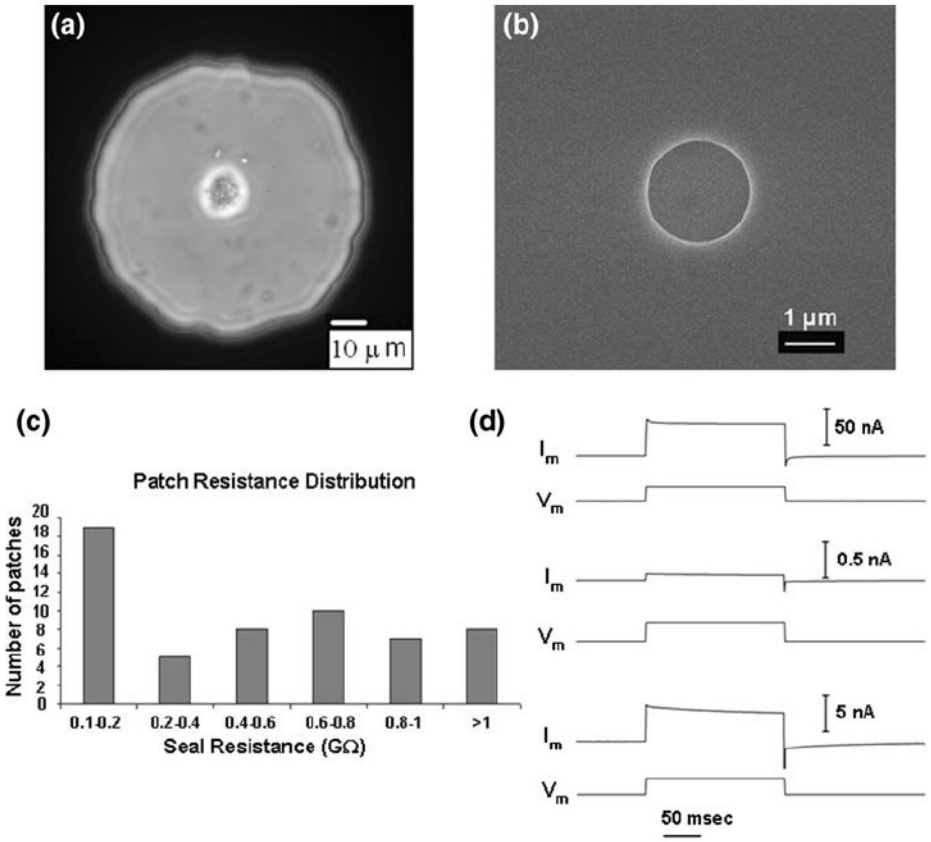

FIGURE 2.

Characterization of the planar patch clamp chip and the assembly: (a) Phase contrast optical microscopy image of a CHO cell sitting over the central pore on the circular SiO_2 membrane window. (b) Scanning electron micrograph of the pore in the silicon dioxide membrane, pore diameter was approximately 2 μm; the scale bar corresponds to 1 μm. (c) Distribution of seal resistance: on cell recording of CHO and PC12 cells seal resistance using 57 different chips. (d) Current (I_m) responses to a 100 mV voltage step (V_m) for: (top) an open pore; (middle) cell plasma membrane forming giga-ohm seal; and (bottom) a whole-cell patch clamp of a CHO cell.

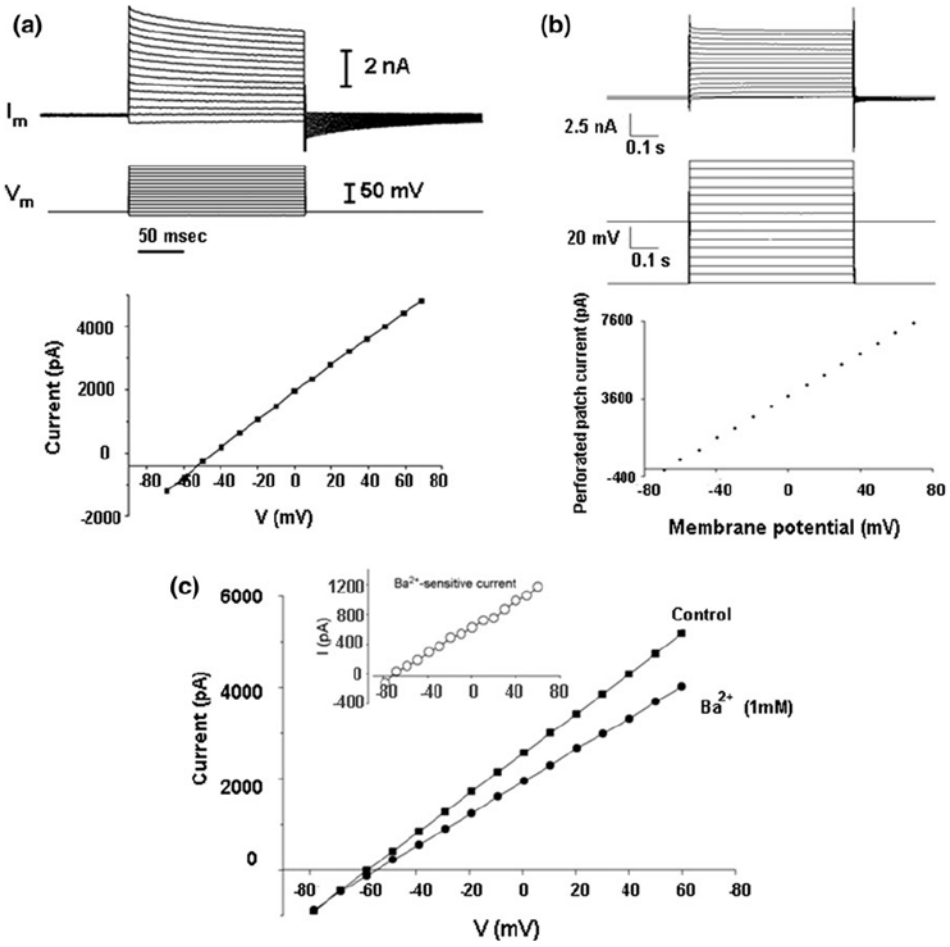

FIGURE 3.

Electrical recordings: (a) Whole cell recording on CHO cells: (top) representative current responses of a CHO cell to step changes of holding potential in whole-cell configuration; (bottom) *I–V* relationship of a CHO cell in whole-cell configuration. (b) Current response of a CHO cell in perforated patch configuration: (top) response to voltage pulses of different magnitude; (bottom) *I–V* relationship 5 min after introduction of amphotericin B in the intracellular solution in cell-attached configuration. (c) *I–V* relationship of a PC12 cell in whole-cell configuration under normal conditions (squares) and after addition of 1 mM $BaCl_2$ (solid circles). Inset: *I–V* relationship for the Ba^{2+}-sensitive current (the difference between current in the absence and the presence of Ba^{2+}) (open circles).

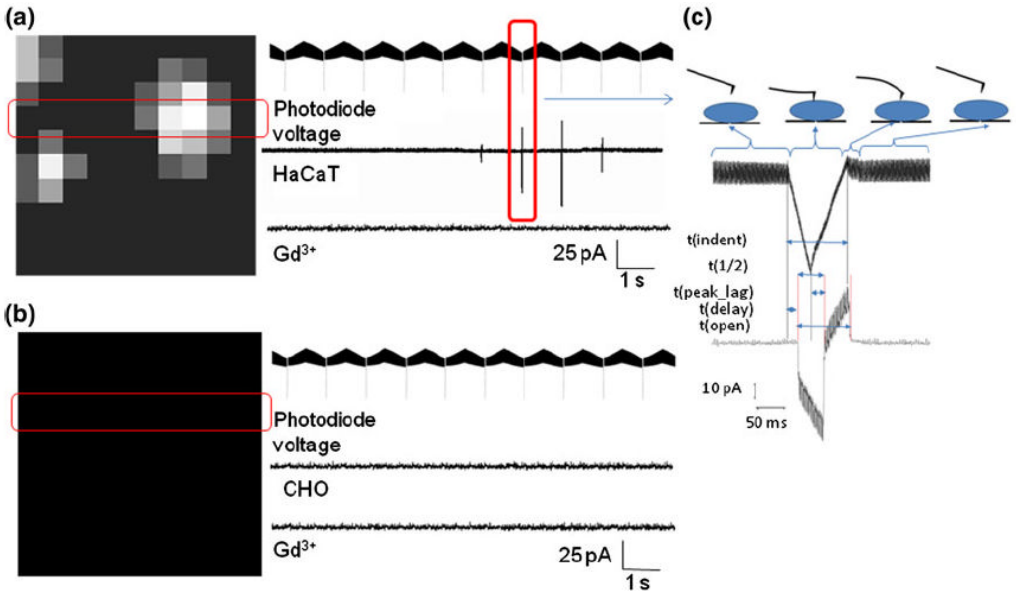

FIGURE 4.

Current map in response to indentation by an AFM cantilever. (a) For HaCaT cell: (left) representative current response to 10 × 10 grid of indentations over a 5 × 5 μm area; (right) voltage output from the AFM photodiode representing cantilever deflection, followed by current response from the highlighted row, followed by the current response from the same row after addition of $GdCl_3$. (b) For CHO cell. (c) High-resolution view of current response for a single indentation. The cartoon on the right shows various stages of cantilever movement corresponding to the photodiode voltage read-out. Parameters: *t*(ind), time over which cantilever is in contact with cell membrane; *t*(1/2), time between onset of current and current peak value; *t*(max_depth), time between the max indentation depth and current peak; *t*(delay), time between membrane contact and onset of current; *t*(i), time over which the channels are open.